Scientific Reports

https://doi.org/10.1038/s41598-026-44968-6

Article in Press

Royal jelly attenuates DMBA induced preneoplastic lesions in rat mammary gland and Skin

Received: 10 October 2025

Accepted: 16 March 2026

Published online: 06 April 2026

Cite this article as: Salehi A., Yaghoobi F., Hosseini S.M. *et al.* Royal jelly attenuates DMBA induced preneoplastic lesions in rat mammary gland and Skin. *Sci Rep* (2026). https://doi.org/10.1038/s41598-026-44968-6

Alireza Salehi, Fatemeh Yaghoobi, Seyed Mohammad Hosseini & Seyedeh-Sara Hashemi

Royal jelly Attenuates DMBA Induced Preneoplastic Lesions in Rat Mammary gland and Skin

Alireza Salehi[1, 2], Fatemeh Yaghoobi[3], Seyed Mohammad Hosseini[3], Seyedeh-Sara Hashemi[2, 4*]

[1]Student Research Committee, Shiraz University of Medical Sciences, Shiraz, Iran

[2] Department of Comparative Biomedical Sciences, School of Advanced Medical Sciences and Technologies, Shiraz University of Medical Sciences, Shiraz, Fars, Iran

[3] Department of Pathology, Bab.C., Babol Branch, Islamic Azad University, Babol, Iran

[4] Burn and Wound Healing Research Center, Shiraz University of Medical Sciences, Shiraz, Iran

* Corresponding author: Seyedeh-Sara Hashemi

Emails and ORCIDs:

Alireza Salehi: Alireza.salehi74@yahoo.com, 0000-0002-3764-8113

Fatemeh Yaghoobi: fatemehyaghoobi6@gmail.com, 0009-0007-6048-0658

Seyed Mohammad Hosseini: dr_hosseini2323@yahoo.com, 0000-0001-6015-3832

Seyedeh-Sara Hashemi: sara_hashemi23@yahoo.com, 0000-0002-0613-6668

Statement of significance

This study highlights royal jelly's potential to mitigate DMBA-induced oxidative and apoptotic damage, offering tissue protection, particularly in

mammary tissue, and suggesting its promise as a natural adjunct in chemoprevention.

Abstract

Background: 7,12-Dimethylbenz[a]anthracene (DMBA) induces reactive oxygen species (ROS) formation, oxidative stress, and apoptosis in target tissues. Royal jelly (RJ) is rich in flavonoids, phenolic acids, and peptides. This study evaluated whether RJ can mitigate DMBA-induced oxidative, apoptotic, and histopathological changes in the rat mammary gland and skin.

Methods: Female Wistar rats were divided into four groups, including the Control (no treatment), RJ (300 mg/kg/week, orally), DMBA (single dose 80 mg/kg, IP), and DMBA + RJ (same doses). After 8 weeks, mammary gland and skin specimens were collected. Oxidative stress markers were quantified in tissue homogenates. Apoptotic gene and protein expression were measured by qRT-PCR and Western blot, respectively. Ki67 expression was assessed by immunohistochemistry. Additionally, histopathological evaluation (H&E stain) was conducted.

Results: DMBA significantly increased MDA, reduced GPx, SOD, and TAC. Pro-apoptotic markers were upregulated, while Bcl2 was downregulated. Histopathology revealed vacuolar degeneration, necrosis, mitotic figures, and corpora amylacea in the mammary gland, and epidermal hyperplasia, mitotic figures, follicular hyperplasia, and focal necrosis in skin. RJ co-treatment restored GPx and SOD levels to almost those of the control group, reduced MDA, decreased p53 and *Bax* to near-control levels, and increased Bcl2 to the approximate level of the control group. Moreover, RJ treatment normalized the mammary gland histologically, while skin showed attenuated necrosis and decreased epidermal hyperplasia and mitotic index.

Conclusions: RJ effectively countered DMBA-induced oxidative stress and apoptosis in the rat mammary gland while preserving tissue integrity. In skin, RJ mitigated oxidative damage and reduced proliferation. These outcomes suggest RJ's potential as an adjuvant antioxidant in glandular disorders, while showing the anticarcinogenic potential.

Keywords: Royal jelly, DMBA, Oxidative stress, Apoptosis, Mammary gland, Skin, Antioxidant

1. Introduction

Cancer is a major global health challenge, arising from complex interactions between genetic predispositions and environmental exposures. Polycyclic aromatic hydrocarbons (PAHs) such as 7,12-dimethylbenz[a]anthracene (DMBA) are well-characterized chemical carcinogens used in preclinical animal models to study tumor initiation in skin and mammary gland [1, 2]. DMBA is bioactivated by cytochrome P450 enzymes that form DNA adducts and generate reactive oxygen species (ROS), leading to oxidative stress, DNA damage, and dysregulated apoptotic signaling [3, 4]. Accumulation of ROS overwhelms endogenous antioxidant defenses, including superoxide dismutase (SOD), and glutathione peroxidase (GPx). This imbalance is reflected in elevated malondialdehyde (MDA), a stable end-product of lipid peroxidation, and reduced activities of SOD/GPx, indicating compromised redox homeostasis [5, 6]. Total antioxidant capacity (TAC) declines further underscore the systemic failure to counteract ROS, exacerbating damage to lipids, proteins, and DNA [7, 8].

Oxidative stress also triggers the intrinsic (mitochondrial) apoptotic pathway. ROS-induced mitochondrial outer membrane permeabilization (MOMP) is mediated by the Bcl-2 family. Pro-apoptotic Bax translocates to mitochondria, promoting cytochrome c release, formation of the apoptosome, and activation of caspase-9 and downstream caspase-3, leading to cell death [9, 10]. Meanwhile, DNA damage stabilizes p53, which transcriptionally upregulates Bax and represses anti-apoptotic Bcl-2, further tipping the balance toward apoptosis. In DMBA-treated rodent models, upregulation of p53, Bax, and caspase-3 and downregulation of Bcl-2 have been consistently observed in mammary glands and skin [9, 11]. Although apoptosis initially removes damaged cells, chronic oxidative stress and apoptotic in non-neoplastic contexts may provoke compensatory proliferation and inflammation, fostering a tumor-promoting microenvironment [12]. Therefore, interventions that attenuate ROS accumulation and modulate apoptotic gene

expression are crucial to preserving tissue integrity during carcinogen exposure. Natural products are promising candidates for such interventions.

Royal jelly (RJ), a honeybee (Apis mellifera) secretion, is rich in proteins, unique peptides, lipids, vitamins, sugars, and diverse polyphenols [13-15]. These constituents confer potent antioxidant, antiproliferative, anti-inflammatory, immunomodulatory, and antimicrobial properties. RJ's flavonoids and phenolic acids scavenge free radicals, while its peptides exhibit synergistic cytoprotective effects [16]. Moreover, RJ directly modulates apoptotic pathways by neutralizing ROS, prevents p53 hyperactivation, and reduces subsequent upregulation of Bax. It was shown that RJ downregulated Bax and upregulated Bcl-2, alongside inhibition of caspase-3 activation and apoptosis via Nrf2/ARE signaling [16]. Similarly, RJ restored Bcl-2, lowered Bax, and reduced caspase-3 activity in cisplatin-treated rat kidneys [17]. These data suggest RJ's dual role: antioxidant and apoptotic regulation, making it a compelling candidate for protecting DMBA-exposed tissues.

This study has mechanistic and translational significance. Understanding RJ's tissue-specific efficacy will elucidate how natural antioxidants protect different epithelial environments from chemical carcinogens. Moreover, delineating RJ's dual roles in antioxidant defense and regeneration may guide clinical application and advocating RJ supplementation for glandular protection during chemotherapy. By integrating molecular and histological aspects, this study provides a comprehensive framework for utilizing RJ in cancer chemoprevention and tissue protection across organ systems.

2. Materials and methods

2.1. Animals and Study Design

This experimental study involved 24 adult female Wistar rats, all 8 weeks old and weighing between 200–220 g. The animals were sourced and housed at the Comparative Medicine and Experimental Center of Shiraz, where they were maintained at a temperature of 20–23°C under a 12-hour light/dark regimen and relative humidity levels of 60–70% [18]. The rats were randomly divided into 4 groups. The first of which was the control group that received normal saline. The second and third groups received oral 300 mg/kg of RJ once a week [19] and a single subcutaneous dose of 80 mg/kg of DMBA, respectively [1, 20]. The fourth group received both compounds with the same dosage.

At the end of the experimental period animals were euthanized by overdose of anesthetic administered intraperitoneally by a cocktail of ketamine at 80 mg/kg (10%, Bremer Pharma GmbH) and xylazine at 10 mg/kg (2%, Alfasan Diergeneesmiddelen BV) [21], followed by sampling tissues. Death was confirmed by permanent cessation of respiratory movements and cardiac activity, absence of corneal and pedal reflexes, and lack of response to toe pinch. Moreover, the ARRIVE guidelines were followed throughout the whole project [22].

2.2. Sampling

Rats were anesthetized, and the tissue samples were immediately obtained and washed with phosphate buffer for the complete removal of any blood stains and clots. Next, half of the tissues were selected randomly to be placed in a 10% formalin buffer solution for 24 hours to be fixated. The other half were homogenized and used for other tests [23].

2.3. Oxidative stress markers

2.3.1. Malondialdehyde (MDA)

MDA is a byproduct of lipid peroxidation, which occurs when ROS attacks cell membranes [24]. Briefly, to estimate MDA using a Nalondi™ Kit (Navand Salamat Lipid Peroxidation Assay Kit), prepared tissue homogenates were added to microplate wells. According to the protocol of the kit, they were incubated with reagents at 95-100°C for 30 minutes. After cooling, absorbance at 532 nm was measured.

2.3.2. Superoxide Dismutase (SOD)

SOD is an enzyme that catalyzes the dismutation of superoxide radicals into hydrogen peroxide and oxygen, thereby reducing ROS levels and protecting cells from oxidative damage [25]. To estimate SOD activity using a Nasdox™ Kit (Navand Salamat Superoxide Dismutase Assay kit), tissue homogenates were prepared. Briefly, they were added to microplate wells, and incubated with reagents at 37°C for 20 minutes according to the kit guideline. The absorbance was measured at 450 nm using a microplate reader.

2.3.3. Glutathione Peroxidase (GPx)

GPx is an enzyme that helps protect cells from oxidative damage by reducing hydrogen peroxide. It plays a crucial role in maintaining the redox balance within cells [26]. To estimate GPx activity using a Nagpix™ Kit (Navand Salamat Glutathione Peroxidase Assay Kit), tissue homogenates were prepared. Briefly, they were added to microplate wells. Next, incubated with reagents at 37°C for 20 minutes. Then, the absorbance at 340 nm using a microplate reader was measured.

2.3.4. Total Antioxidant Capacity (TAC)

TAC measures the overall ability of a biological sample to neutralize ROS and other free radicals. It reflects the cumulative action of all antioxidants present in the sample [25]. To measure TAC using a Naxifer™ Kit (Navand Salamat Total Antioxidant Capacity Assay Kit), tissue homogenates were prepared. Next, the sample was added to microplate wells, then the ABTS solution was added, and hydrogen peroxide solution was used to initiate the reaction. The kit was incubated at room temperature for 20 minutes. Finally, the absorbance at 414 nm was measured using a microplate reader.

2.4. PCR Real-time

To estimate Bax, Bcl2, P53, and Caspase 3 gene expressions in rat tissue homogenates using cDNA and PCR, first RNA from the tissue samples was extracted and cDNA was synthesized using reverse transcriptase. Specific primers for the genes were designed and PCR was performed to amplify the target cDNA. The PCR products were analyzed using real-time PCR to quantify the gene expression levels [27, 28]. (Table 1)

Table 1. Primer sequences and sizes.

Gene	Forward Primer	Reverse Primer	Size (bp)
Bax	GTTGCCCTCTTCTACTTTGC	GTTCTGATCAGTTCCGGCAC	200
Bcl2	AGTTCGCCGAGATGTCCAG	AGCCAGGAGAAATCAAACAGAG	220
P53	CAGCCAAGTCTGTGACTTGC	CTGCTTGCATTCTGGGACAG	180
Caspase 3	GACTGGACTGTGGCTGTGAT	CGCATACTTCTGTCATGCCG	210

2.5. Western blotting

During tissue collection, a 1 g sample of colon from each experimental group was gathered and homogenized in RIPA buffer (approximately 3 mL of cold buffer per gram of tissue) using a mechanical homogenizer (Tissue Mini Grinder, Model TD 1000) on ice to ensure optimal cell lysis and protein solubilization. Following homogenization, lysates were centrifuged at 12,000 rpm for 10 minutes at 4 °C to pellet debris, and supernatants were collected for subsequent analysis. Protein concentrations were quantified to normalize loading volumes, then equal amounts (20–30 µg) of each sample were loaded onto SDS-PAGE gels and transferred onto PVDF membranes using a tank blotting system (Electrophoresis Western Blotting Tank, Model WPN-80) under a constant current of 100 V for 90 minutes to achieve efficient protein transfer. Membranes were blocked with BSA in Tris-buffered saline containing 0.1% Tween-20 for 1 hour at room temperature, then incubated overnight at 4 °C with primary antibodies against Bax, Bcl2, P53, Caspase 3, and β-actin (Housekeeping protein) at manufacturer-recommended dilutions to detect target proteins. β-actin served as an internal normalization reference for densitometric analyses. After primary incubation, membranes were washed three times in TBS-T and probed with appropriate HRP-conjugated secondary antibodies for 1 hour at room temperature, followed by further washes in TBS-T. Quantitative densitometry was performed in ImageJ by measuring the gray-scale intensity of each protein band. The area under each band was calculated and divided by the corresponding β-actin signal to yield normalized expression values for Bax, Bcl2, P53, and Caspase 3 in each sample [29].

2.6. Immunohistochemical evaluation

Tissues were obtained from rats, fixed in 10% buffered formalin, and routinely processed for paraffin embedding. Sections were cut at 5 µm

thickness, deparaffinized, and rehydrated. Endogenous peroxidase activity was blocked for 5 minutes, followed by a 20-minute incubation with a protein blocking solution. Antigen retrieval was then carried out using citrate buffer in a decloaking chamber (Biocare, Concord, CA, USA) at 125°C for 30 seconds. Next, the sections were incubated with a prediluted anti-Ki67 antibody (Biocare, Concord, CA, USA), and then treated with an HRP-tagged polymer detection system (Mach 3, Biocare). The chromogenic reaction was developed using diaminobenzidine to visualize the staining [30].

2.7. Histopathological examination

For the histopathological evaluation, tissue samples were first rinsed with sterile saline and then immersed in 10% formalin for fixation (DS2080/H, Did Sabz Co.). The tissues were subsequently dehydrated and embedded in paraffin using TE100 embedding cassettes (Pouya Abzar Azma). Once the blocks had solidified and cooled, 5-µm sections were cut (DS4055, Did Sabz Co.), stained with hematoxylin and eosin (H&E), and examined under an Olympus CX21 light microscope. Histopathological comparisons among groups were performed based on the qualitative scoring method [31].

2.8. Data analysis

Statistical analyses were conducted with SPSS version 27 (USA software, version 27, IBM Corp.). Data were evaluated using one-way ANOVA, and significant differences between groups were identified through Tukey post hoc test. A p-value below 0.05 was considered statistically significant [32]. Additionally, the histopathological evaluation scored the severity of tissue damage as no lesion (-), mild lesions (+), moderate lesions (++), and severe lesions (+++) [32].

3. Results

3.1. Oxidative stress markers

3.1.1. Mammary gland

As shown in Figure 1, animals treated with DMBA exhibited an imbalance in redox status compared to the control group. Specifically, GPx activity decreased in the DMBA group compared to the control group, while MDA levels rose significantly. Similarly, SOD activity rose in DMBA-treated rats significantly, and TAC declined relative to control significantly. In the DMBA + RJ group, GPx activity decreased compared to DMBA but remained slightly higher than control levels. MDA concentrations in the DMBA + RJ group dropped significantly relative to DMBA, although they did not fully return to baseline. SOD values fell close to control in the DMBA + RJ group, and TAC likewise improved significantly versus DMBA. RJ group only altered the TAC significantly compared to control. (Figure 1)

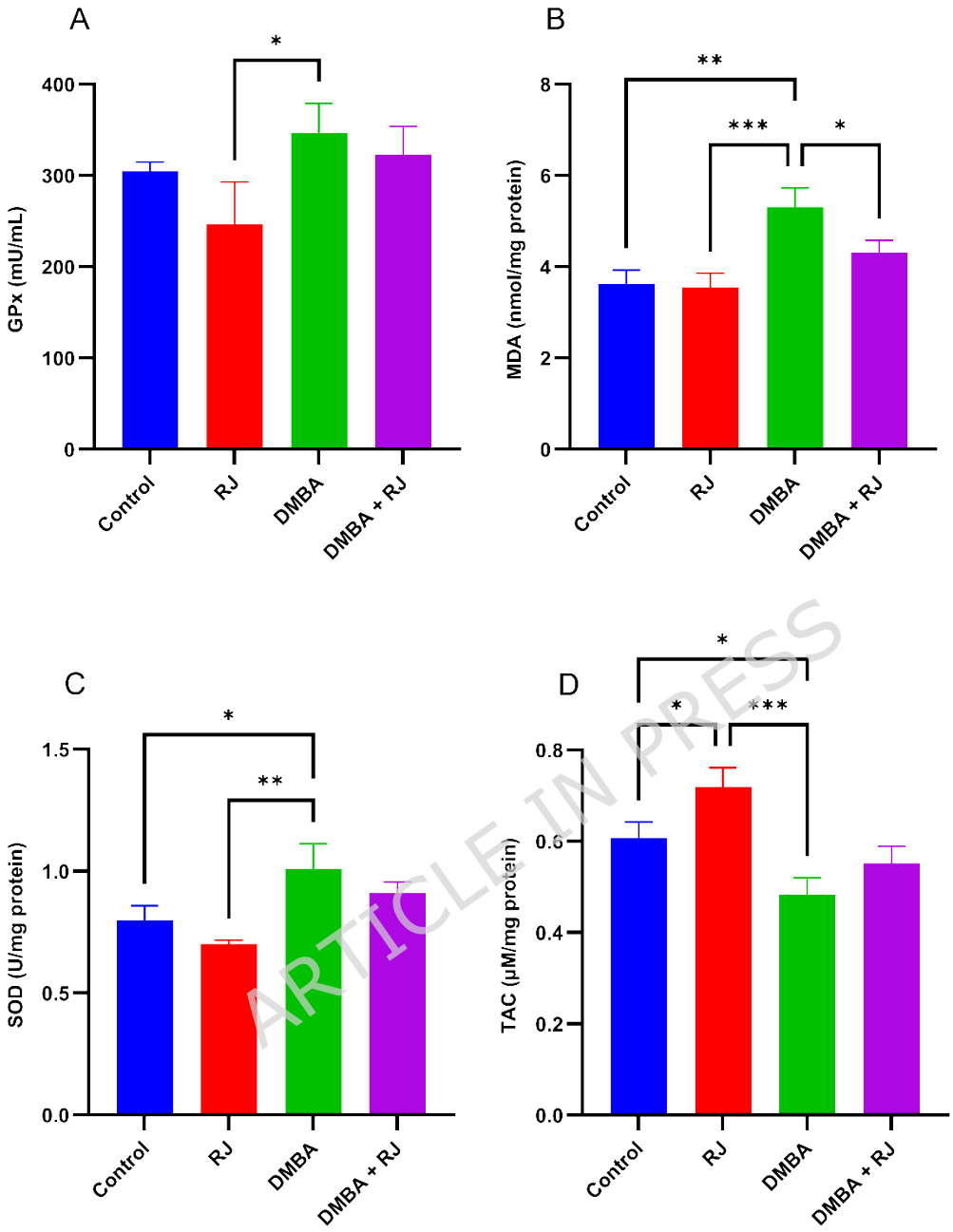

Figure 1. Mammary gland tissue oxidative markers levels. A: Glutathione peroxidase levels. B: Malondialdehyde levels. C: Superoxide dismutase levels. D: Total Antioxidant Capacity levels. Significant differences between groups are shown with * P<0.05, ** P<0.01, *** P<0.001, and **** P<0.0001.

3.1.2. Skin

DMBA induced a significant elevation in MDA and a reduction in antioxidant enzymes. GPx and SOD both significantly increased compared to the control group. TAC values in the DMBA group fell significantly compared to the control group. DMBA + RJ significantly attenuated these changes, including fell back of GPx to nearly normal level from the control group, MDA was reduced significantly compared to the DMBA group, SOD activity reduced to near-control values, and TAC improved substantially compared to DMBA, although remained slightly lower than the control group. The RJ group again showed only a significant difference from control in the TAC marker. (Figure 2)

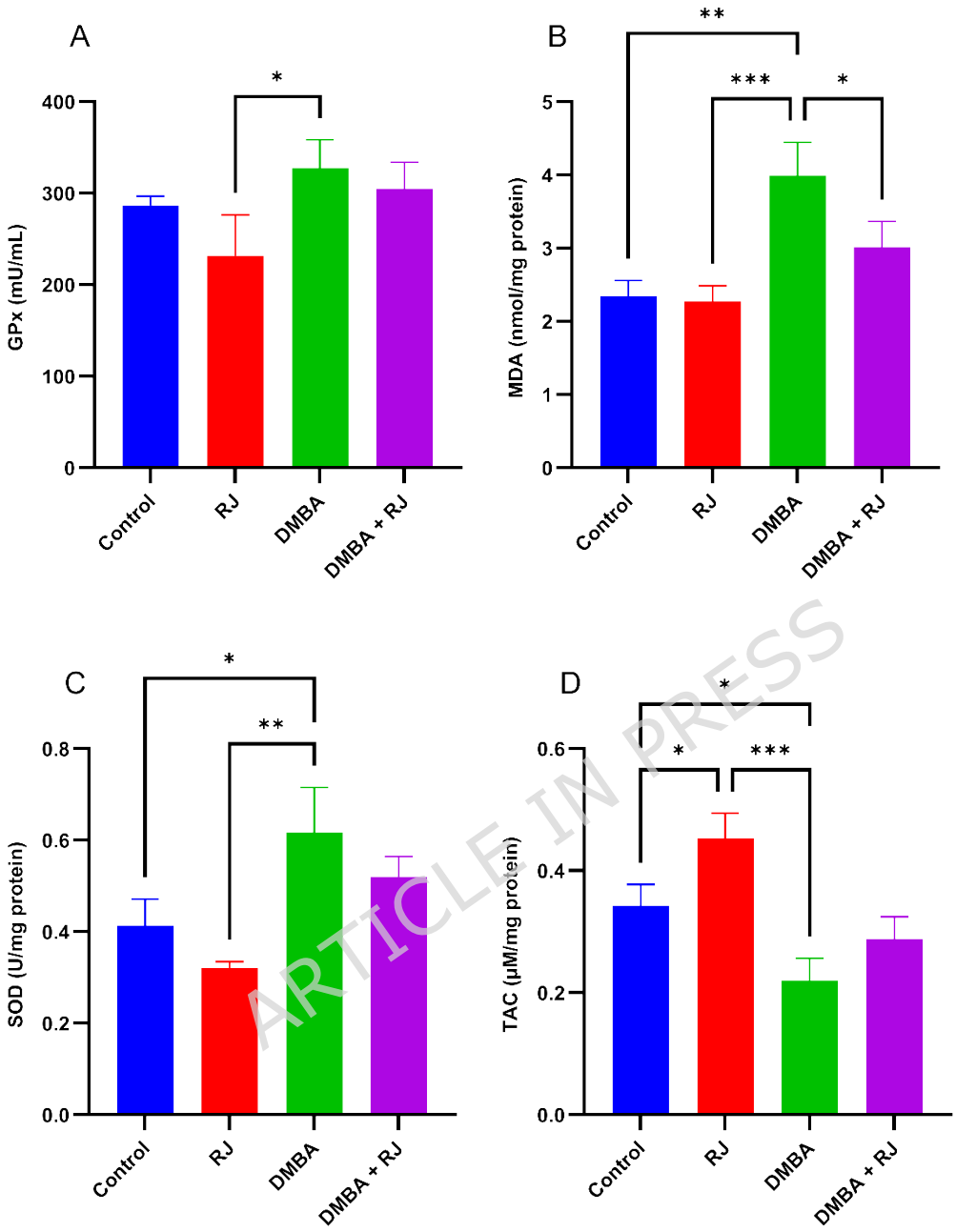

Figure 2. Skin tissue oxidative markers levels. A: Glutathione peroxidase levels. B: Malondialdehyde levels. C: Superoxide dismutase levels. D: Total Antioxidant Capacity levels. Significant differences between groups are shown with * P<0.05, ** P<0.01, and *** P<0.001.

3.2. Apoptosis pathway genes expression

3.2.1. Mammary gland

As depicted, DMBA treatment significantly upregulated the pro-apoptotic Bax and Caspase 3 genes compared to the control group. The tumor suppressor P53 also increased significantly compared to the control group. Conversely, Bcl2 levels declined significantly in the DMBA group in comparison to the control group. When RJ was administered alongside DMBA, Bax and Caspase 3 expressions levels fell significantly compared to the DMBA group and P53 levels significantly reduced to near-control values. Moreover, Bcl2 level moderately increased in the DMBA + RJ group compared to the DMBA group. The RJ group did not differ significantly from the control group. (Figure 3)

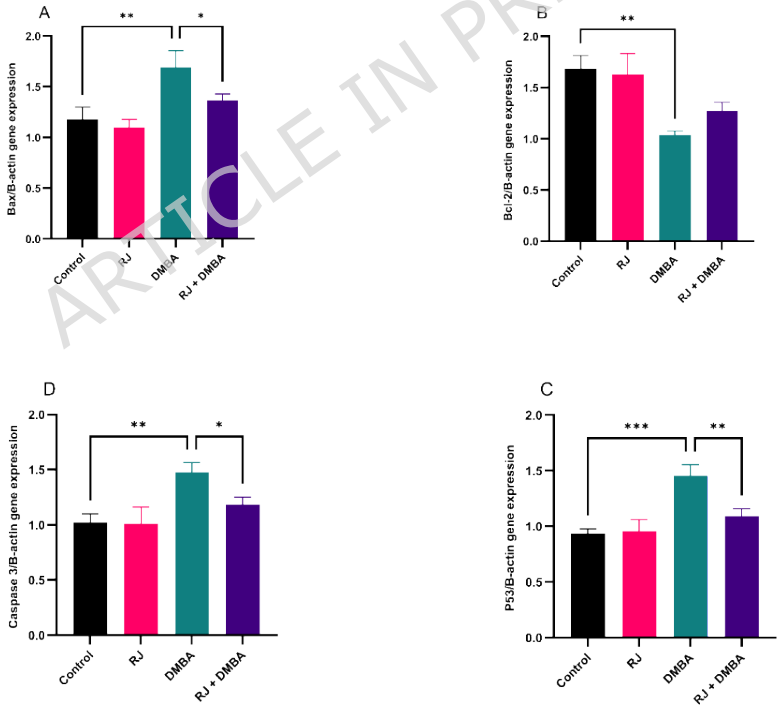

Figure 3. Mammary gland tissue gene expression levels. A: Bax/B-actin gene. B: Bcl2/B-actin gene. C: Caspase 3/B-actin gene. D: P53/B-actin gene.

Significant differences between groups are shown with * $P<0.05$, ** $P<0.01$, and *** $P<0.001$.

3.2.2. Skin

In skin, Bax and Caspase 3 levels rose significantly in the DMBA group. Additionally, P53 level increased significantly compared to the control group. In contrast, Bcl2 declined significantly compared to the control group. Co-administration of RJ with DMBA significantly mitigated these changes, including the reduction of Bax, Caspase 3, and P53 expression levels. However, Bcl2 expression was increased compared to the DMBA group. Again, RJ treatment did not significantly alter gene expression compared to the control group. (Figure 4)

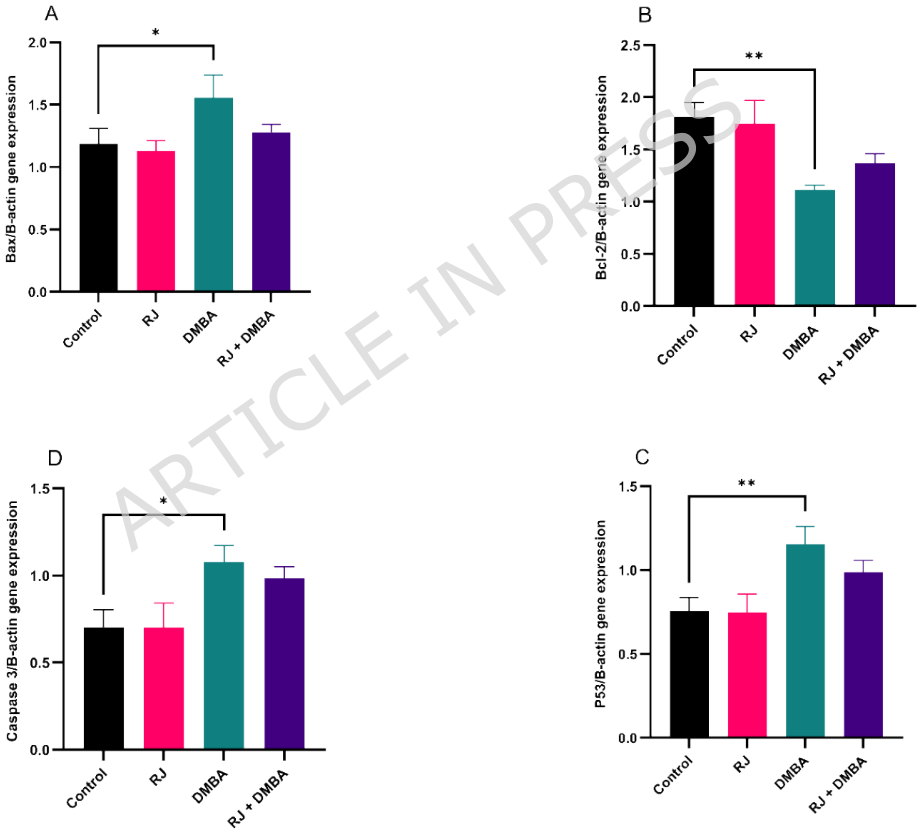

Figure 4. Skin tissue gene expression levels. A: Bax/B-actin gene. B: Bcl2/B-actin gene. C: Caspase 3/B-actin gene. D: P53/B-actin gene. Significant differences between groups are shown with * P<0.05, ** P<0.01, and *** P<0.001.

3.3. Apoptosis pathway proteins expression

3.3.1. Mammary gland

In the DMBA group, Bax, P53, and Caspase 3 levels significantly increased, while Bcl2 decreased compared to the control group. Compared to the DMBA group, the Bax level fell, Caspase 3 decreased, P53 reduced, and Bcl2 increased in the DMBA + RJ group. (Figures 5)

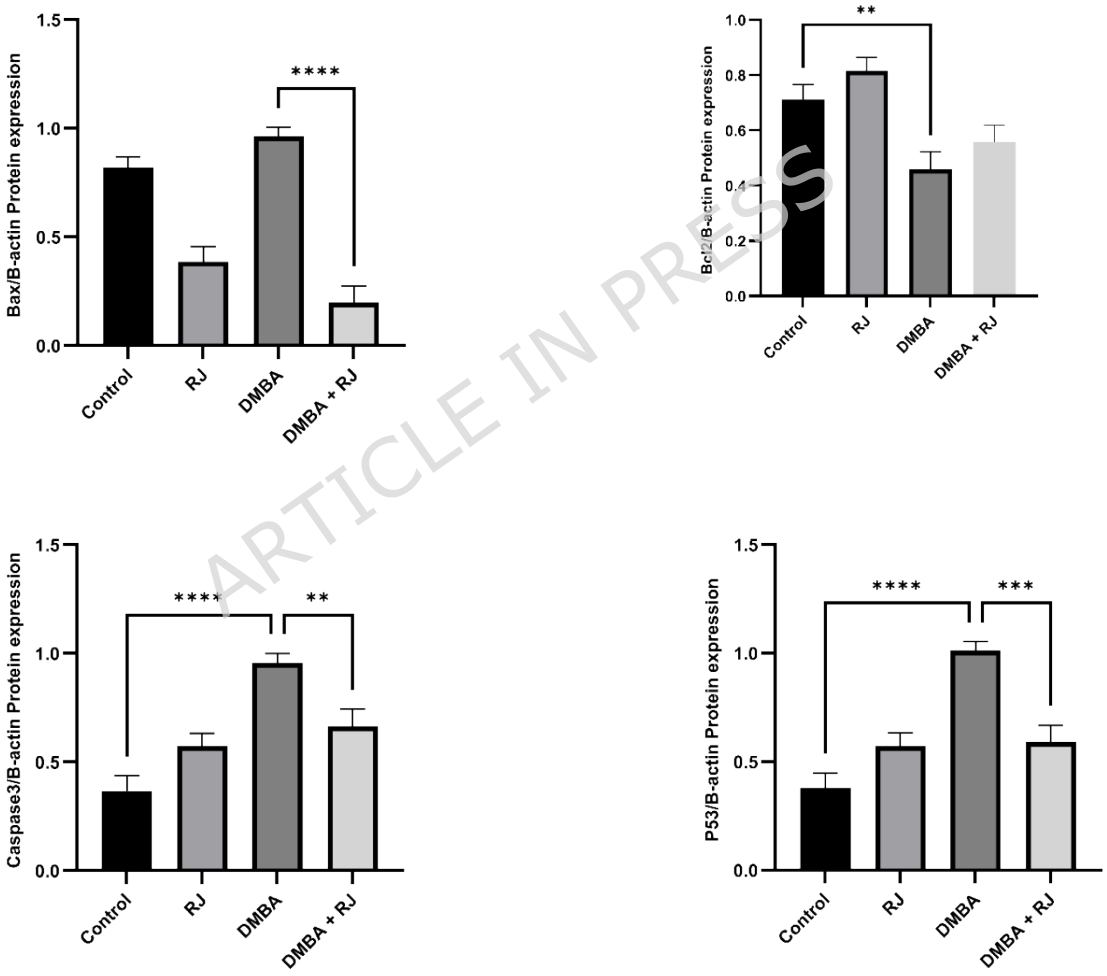

Figure 5. Mammary gland tissue protein expression after western blot analysis of the gel bands in gray scale. Significant differences between

groups are shown with * P<0.05, ** P<0.01, *** P<0.001, and **** P<0.0001.

3.3.3. Skin

Similarly, DMBA induced significant elevations in Bax, Caspase 3, and P53, while Bcl2 protein declined significantly. Co-treatment with RJ brought Bax and Caspase 3 down significantly compared to the DMBA group, reduced P53 significantly, and moderately increased Bcl2 level compared to the DMBA group. No significant differences were observed between the RJ and control groups. (Figures 6)

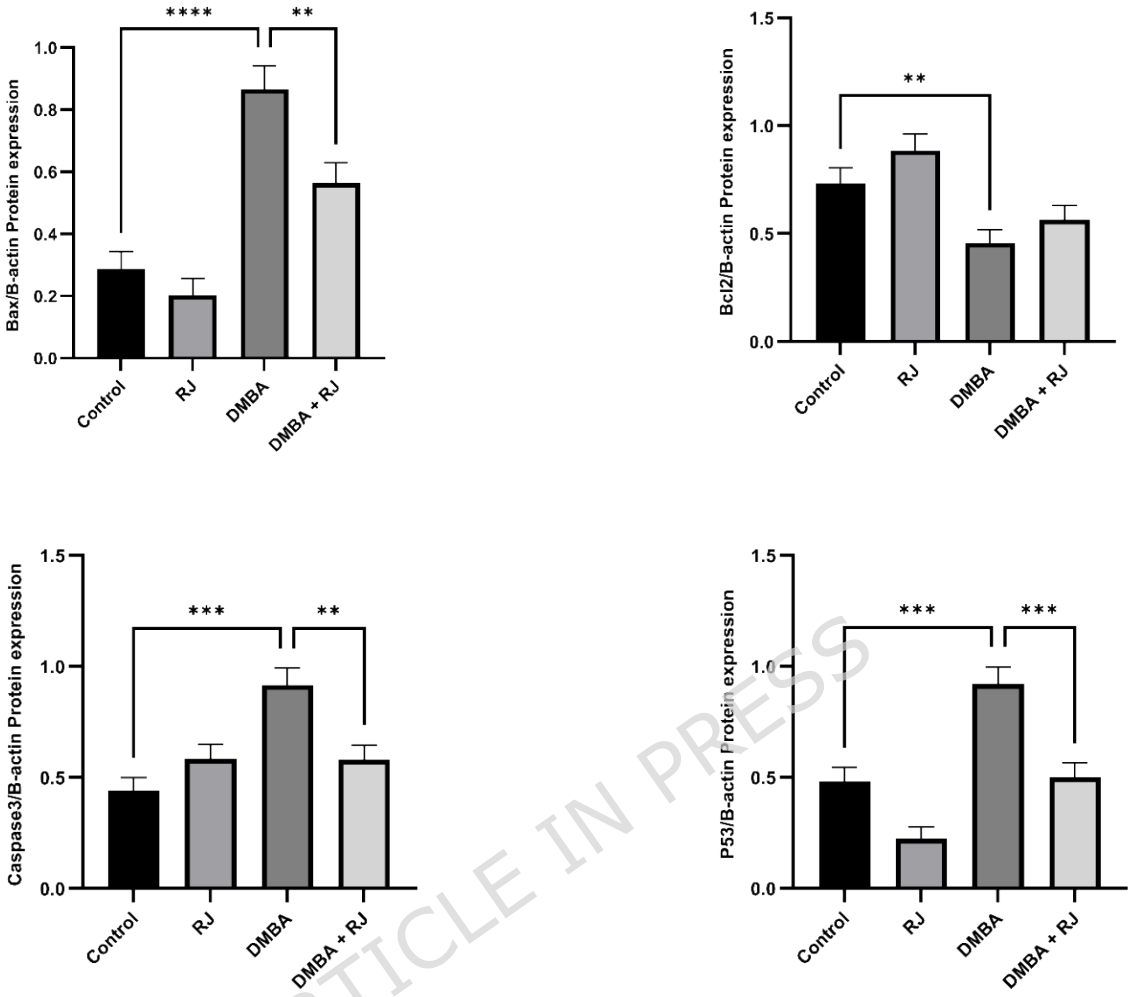

Figure 6. Skin tissue protein expression after western blot analysis of the gel bands in gray scale. Significant differences between groups are shown with * P<0.05, ** P<0.01, *** P<0.001, and **** P<0.0001.

3.4. Ki-67 expression

3.4.1. Mammary gland

In the mammary gland, Ki67 immunostaining revealed no noticeable expression in both the Control and RJ groups. In contrast, the DMBA group exhibited markedly elevated Ki67 expression, with numerous intense nuclear stains throughout the ductal and lobular epithelium, reflecting DMBA-induced proliferation and hyperplasia. However, the DMBA + RJ group showed reduced Ki67 expression to a moderate level, with fewer and less intensely stained nuclei compared to the DMBA group. (Table 2 and Figure 7)

Table 2. Mammary gland Ki67-expressing cells. The severity of expressing cells is shown by no lesion (-), mild lesions (+), moderate lesions (++), and severe lesions (+++).

Groups	Intracellular Ki67 expression
Control	-
RJ	-
DMBA	+++
DMBA + RJ	++

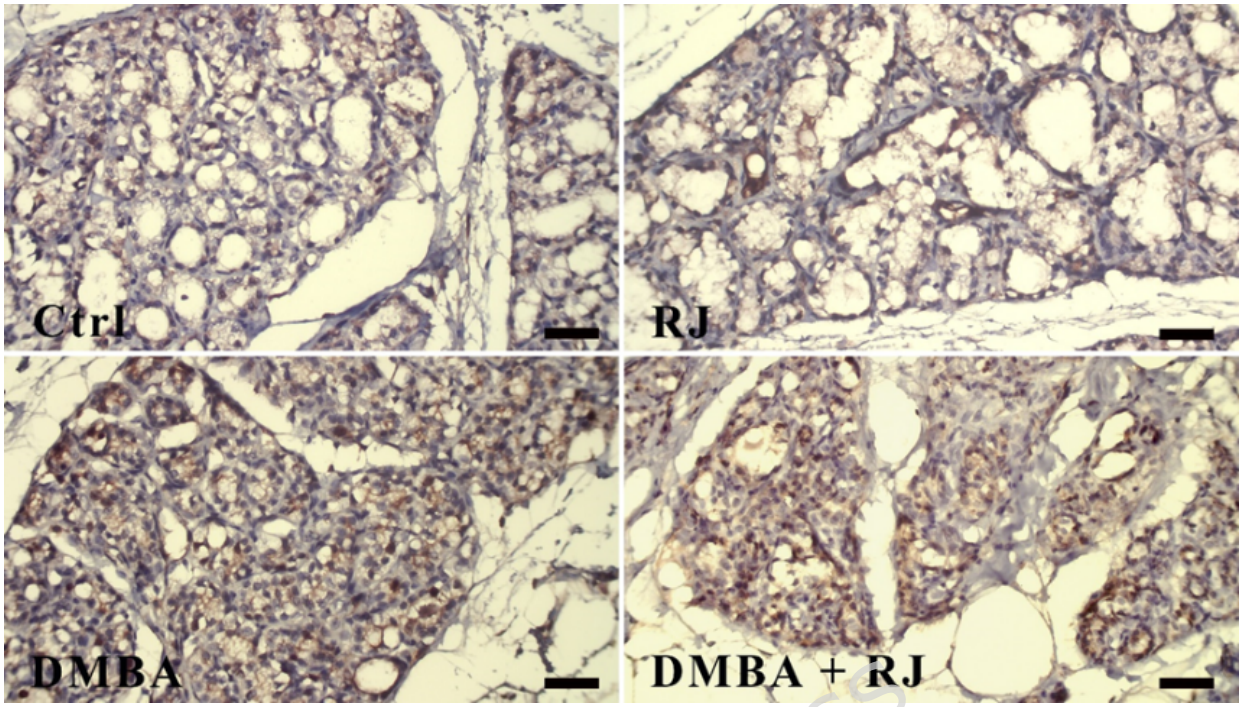

Figure 7. Mammary gland tissue IHC examination. Normal tissue conditions in the control and RJ groups. Increased Ki67-expressing cells in other groups. X40 magnification. Ki67 immunohistochemical staining, Scale bar: 50 um.

3.4.2. Skin

In skin sections, Ki67 immunostaining showed minimal proliferative activity in the Control and RJ groups, with only rare basal keratinocyte nuclei were labeled. DMBA exposure produced a moderate increase in Ki67-positive keratinocytes, especially within the basal and dermis layers of the interfollicular layer, indicating initiation of hyperproliferative, potentially preneoplastic damage. When RJ was co-administered with DMBA, Ki67 expression reduced to a mild level, suggesting that RJ counteracted DMBA-driven keratinocyte proliferation (Table 3 and Figure 8).

Table 3. Mammary gland Ki67-expressing cells. The severity of expressing cells is shown by no lesion (-), mild lesions (+), and moderate lesions (++).

Groups	Intracellular Ki67 expression
Control	-
RJ	-
DMBA	++
DMBA + RJ	+

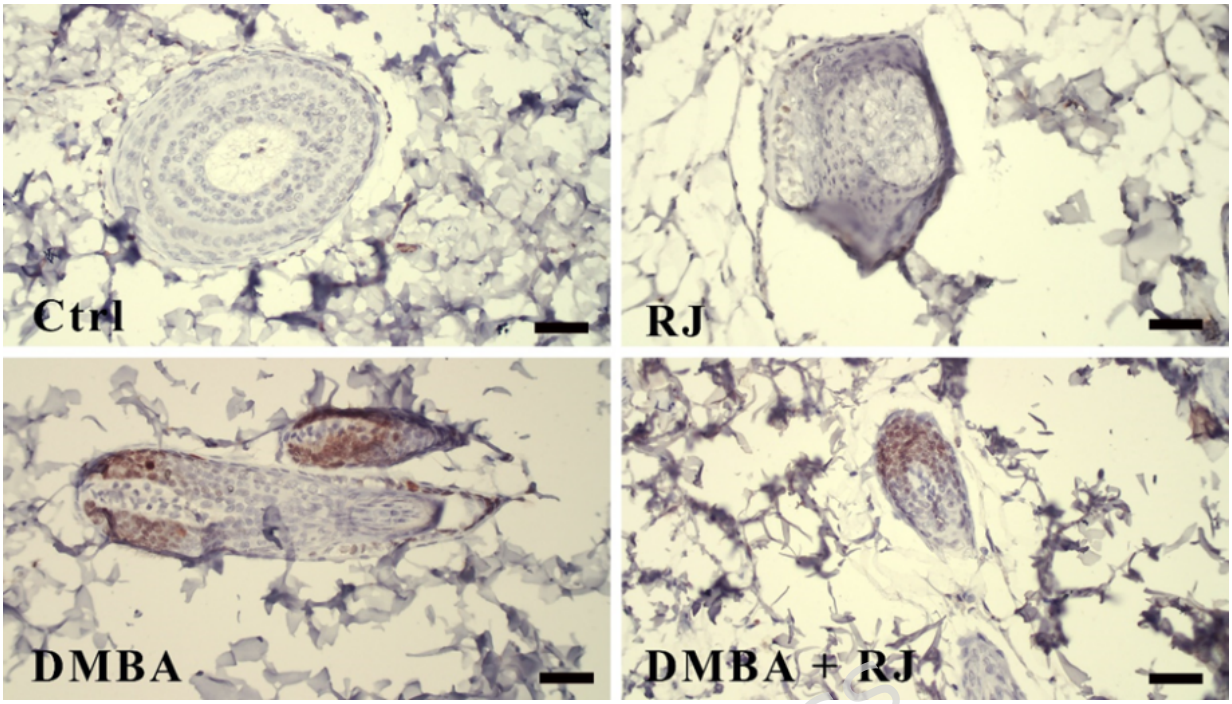

Figure 8. Skin tissue IHC examination. Normal tissue conditions in the control and RJ groups. Increased Ki67-expressing cells in other groups. X40 magnification. Ki67 immunohistochemical staining, Scale bar: 50 um.

3.5. Histopathological examination

3.5.1. Mammary gland

In both control and RJ groups, normal lobuloalveolar architecture was preserved, with no vacuolar changes, mitotic figures, necrosis, or corpora amylacea. In contrast, the DMBA group showed severe histopathological alterations, including mild vacuolar degeneration of glandular epithelial cells, moderate mitotic figures, focal necrotic areas, and number of corpora amylacea within dilated ducts and lobules. Administration of RJ alongside DMBA improved the tissue condition with reducing vacuolar degeneration, mitotic figures, necrotic focals, and corpora amylacea compared to the DMBA group. (Table 4 and Figure 9)

Table 4. Mammary gland tissue damage indices. The severity of damage is shown by no lesion (-), mild lesions (+), and moderate lesions (++).

Groups	Necrosis	Vacuole degeneration	Mitotic figures	Corpora amylacea
Control	-	-	-	-
RJ	-	-	-	-
DMBA	++	+	++	++
DMBA + RJ	+	-	+	+

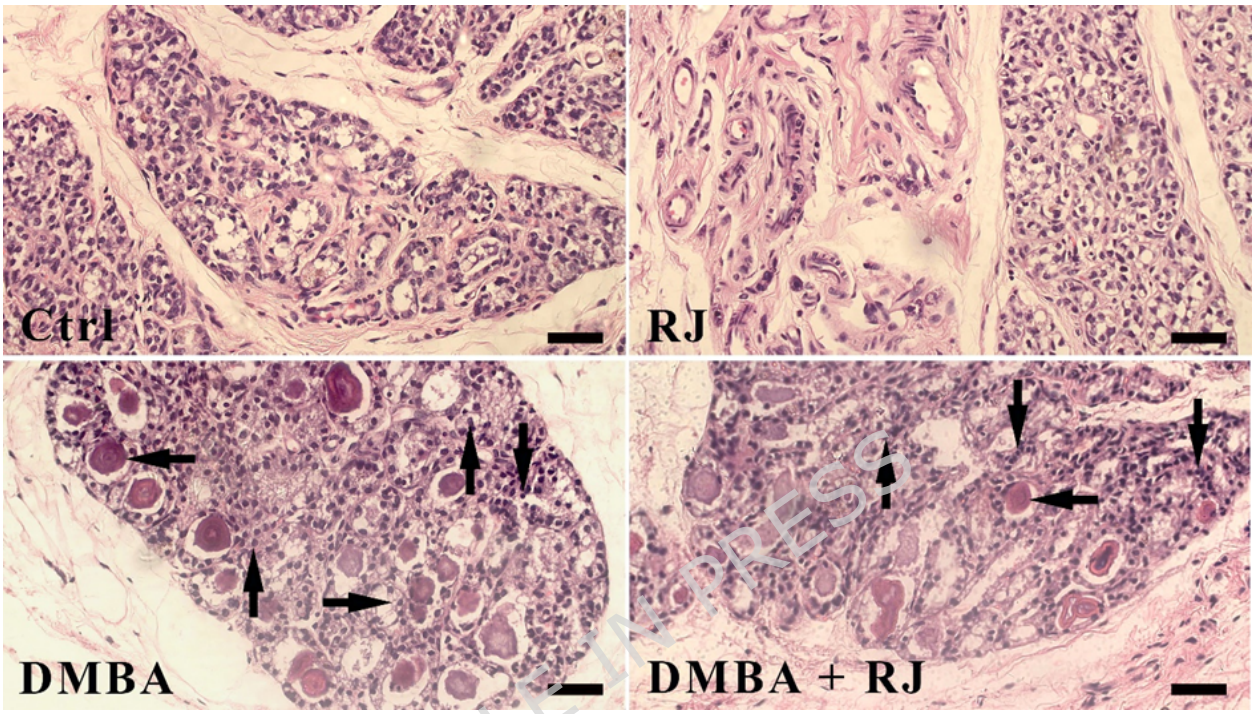

Figure 9. Mammary gland tissue histopathology. Normal tissue conditions in control and RJ groups. Vacuolar degeneration (Right arrow), mitotic figures (Upward arrow), necrosis (Downward arrow), and Corpora amylacea (Left arrow) were observed in both DMBA and DMBA + RJ groups. Magnification X40. H&E staining.

3.5.2. Skin

Control and RJ groups maintained normal epidermal and dermal architecture, with no pathological changes. In DMBA-treated rats, moderate mitotic figures, severe hair follicle hyperplasia, and moderate number of focal necrotic areas were observed. In contrast, the DMBA + RJ group exhibited a significant improvement, such as reduction of mitotic figures to mild, substantial decrease of hair follicle hyperplasia, and reduced focal necrotic areas. (Table 5 and Figure 10)

Table 5. Skin tissue damage indices. The severity of damage is shown by no lesion (-), mild lesions (+), moderate lesions (++), and severe lesions (+++).

Groups	Necrosis	Hair follicle hyperplasia	Mitotic figures
Control	-	-	-
RJ	-	-	-
DMBA	++	+++	++
DMBA + RJ	+	+	+

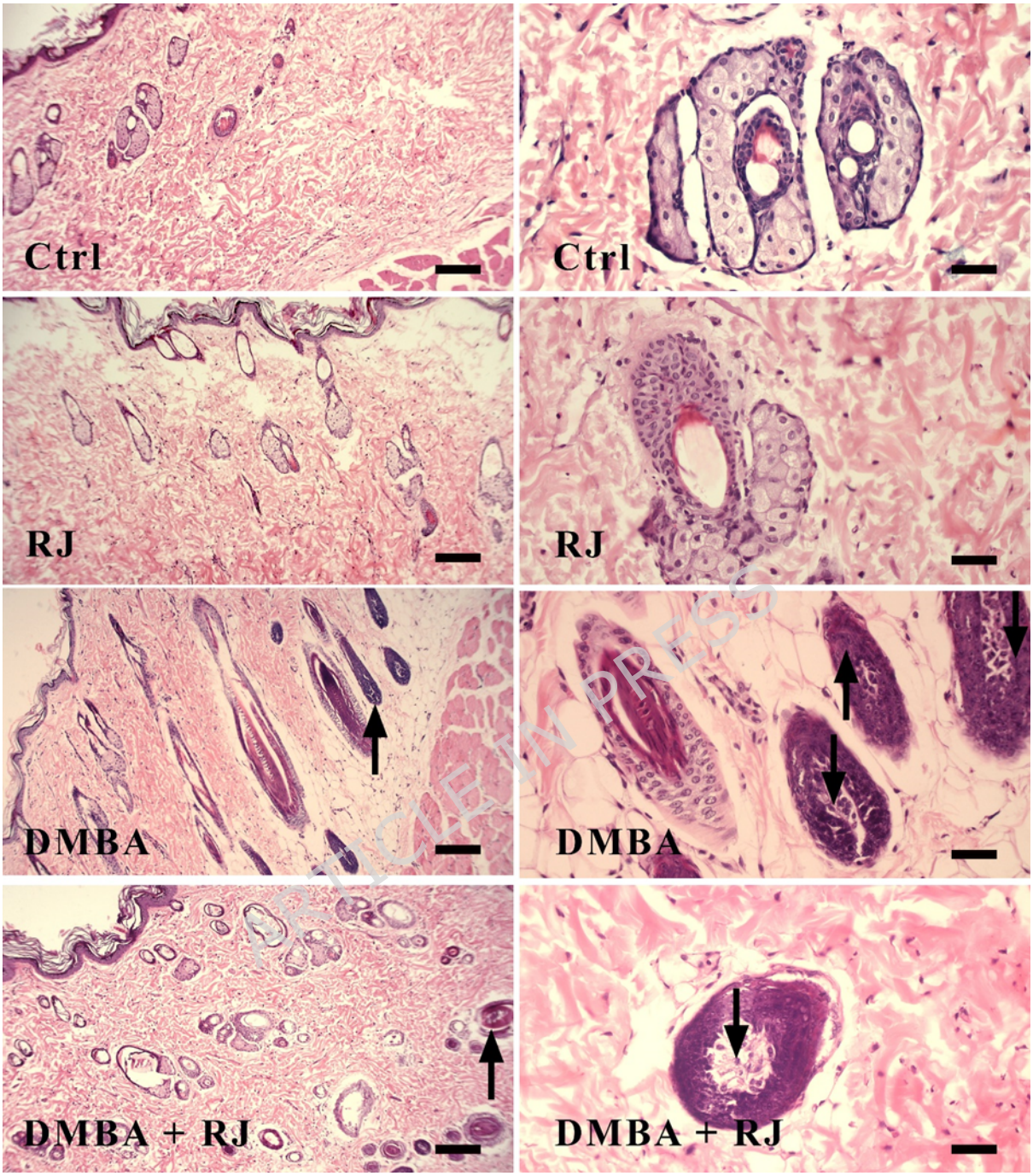

Figure 10. Skin tissue histopathology. Normal tissue conditions in the control and RJ groups. Hair follicle hyperplasia (upward arrow) and mitotic figures (downward arrow) were observed in both DMBA and DMBA + RJ groups. Magnification X40. H&E staining.

4. Discussion

This study investigated the protective effects of RJ against DMBA-induced oxidative stress, apoptosis, and histopathological alterations in mammary gland and skin. Briefly, our data demonstrated that DMBA exposure triggers significant redox imbalance, upregulates pro-apoptotic signaling, downregulates anti-apoptotic factors, and produces marked histological damage, causing proliferation and hyperplasia in both tissues. Co-treatment with RJ reversed these molecular and biochemical changes and brought the near-normal condition in both tissues.

DMBA is metabolized by cytochrome P450 enzymes into diol-epoxide intermediates that generate ROS, leading to oxidative stress in target tissues such as mammary gland and skin. Elevated levels of MDA indicate increased lipid peroxidation and oxidative stress [24]. Thus, lower level suggests reduced oxidative damage and better cellular integrity. Elevated ROS levels induce lipid peroxidation, as evidenced by increased MDA, and deplete endogenous antioxidant enzymes like SOD and GPx [33, 34]. An increase in GPx activity typically indicates an enhanced antioxidant defense mechanism, suggesting the organism is responding to oxidative stress [25, 26]. Conversely, a decrease might suggest a compromised antioxidant system, making the organism more susceptible to oxidative damage. In the mammary gland, DMBA decreased GPx, SOD, and TAC, while skin tissue exhibited a decline in GPx, SOD, and TAC compared to the control group. Increased SOD activity suggests an upregulated antioxidant defense system, indicating the organism is combating oxidative stress [25]. A decrease in SOD activity may indicate a weakened defense mechanism, leading to higher susceptibility to oxidative damage. In addition, an increase in TAC indicates a stronger antioxidant defense system, suggesting better protection against oxidative stress [25]. A decrease in TAC suggests a weakened antioxidant system, making the organism more vulnerable to oxidative damage. These alterations align with prior findings that DMBA-induced ROS accumulation compromises

antioxidant defenses, resulting in oxidative damage and subsequent lipid, protein, and DNA oxidation [35].

RJ contains a range of bioactive constituents, including flavonoids, phenolic acids [19], and unique peptides, that scavenge free radicals and upregulate endogenous antioxidant enzymes via activation of the Nrf2 pathway [16, 36]. Consistent with these mechanisms, RJ co-treatment restored GPx and SOD activities close to control values in both tissues and reduced MDA levels in mammary gland and skin relative to DMBA group. RJ also improved TAC in mammary and skin tissue. Similar antioxidant protective effects of RJ have been reported in other models. Rizki et al. showed RJ increased glutathione levels and decreased lipid peroxidation by enhancing GPx and SOD in preconception female rats [37], while RJ's efficacy in mitigating DNBS-induced colitis via upregulating SOD and GPx was demonstrated. Collectively, these data underscore that RJ's antioxidant properties mediated by direct radical scavenging and Nrf2-mediated transcriptional activation of antioxidant defenses are central to counteracting DMBA-induced oxidative stress in mammary gland and skin tissues.

Oxidative stress not only damages cellular macromolecules but also triggers apoptosis through the mitochondrial pathway. ROS facilitate mitochondrial outer membrane permeabilization (MOMP) by upregulating pro-apoptotic proteins like Bax and promote cytochrome c release into the cytosol [33, 38]. Bax is a pro-apoptotic gene that promotes programmed cell death [39, 40]. Higher levels of Bax indicate enhanced apoptosis, which might occur in response to cellular stress or DNA damage. This can be beneficial in eliminating damaged or cancerous cells. Lower levels of Bax suggest reduced apoptosis, which may contribute to uncontrolled cell proliferation and tumor development. Released cytochrome c activates Caspase 3, culminating in apoptotic cell death. Concurrently, ROS-induced DNA damage stabilizes and activates the tumor suppressor p53, which transcriptionally upregulates Bax and represses Bcl2, tipping the balance toward apoptosis. Bcl-2 is an anti-

apoptotic gene that inhibits apoptosis and promotes cell survival by preventing the release of cytochrome c from mitochondria [40]. Elevated Bcl-2 levels can lead to prolonged cell survival, which is often seen in cancerous cells. This might indicate resistance to apoptosis-inducing treatments. Reduced Bcl-2 levels can increase apoptosis, which might be beneficial in cancer therapies aimed at inducing cell death in tumor cells.

In our study, DMBA significantly increased mRNA and protein levels of Bax, Caspase 3, and p53 while decreasing Bcl2 in mammary gland and skin compared to the control group. These findings are consistent with an earlier reported that showed elevated p53 and Bax expression in DNA adduct formation and oxidative damage [35]. Similarly, in skin, it was demonstrated that PAH metabolites like DMBA provoke p53-mediated apoptosis in keratinocytes via ROS generation. P53 is a tumor suppressor gene that plays a crucial role in regulating the cell cycle, DNA repair, and apoptosis. It helps prevent the proliferation of cells with damaged DNA. Higher levels of P53 usually indicate a response to DNA damage and can lead to cell cycle arrest or apoptosis, serving as a protective mechanism against cancer. Lower levels or mutations in P53 can result in the failure to control cell proliferation, contributing to tumorigenesis. RJ co-treatment reduced Bax and Caspase 3 compared to the control in both tissues and normalized p53 expression, while restoring Bcl2 to near level of control. Caspase 3 is an executioner caspase in the apoptosis pathway and is responsible for cleaving various cellular substrates, leading to the morphological and biochemical changes associated with apoptosis. Elevated Caspase 3 activity indicates increased apoptosis, which can be a response to therapeutic treatments or cellular stress. Reduced Caspase 3 activity suggests impaired apoptotic processes, which may be associated with resistance to apoptosis in cancer cells. The anti-apoptotic effect of RJ likely involved multiple mechanisms, including attenuation of ROS levels through antioxidant action prevents p53 hyperactivation and mitochondrial permeabilization, enhancing the Nrf2/ARE pathway,

upregulating cytoprotective genes that indirectly suppress pro-apoptotic signaling [16, 36], and directly modulating apoptotic regulators. It was previously shown that RJ downregulates Bax and upregulates Bcl2 in rats, preventing renal apoptosis [16, 34]. Therefore, RJ's ability to both decrease ROS and directly influence apoptotic gene transcription underlies the observed reversal of DMBA-induced apoptosis in mammary and skin tissues.

Ki67 is a nuclear antigen expressed exclusively during active phases of the cell cycle, making it a robust marker of cellular proliferation. Treatment with RJ reduced the expression of Ki67, which signifying partial attenuation of proliferative signaling in both mammary and skin tissues. In both tissues, DMBA markedly enhanced Ki67-mediated proliferation compared to the Control and RJ groups. In the mammary gland, the upregulated Ki67 expression following DMBA aligned with prior reports that DMBA induces rapid lobuloalveolar hyperplasia and tumor initiation, evidenced by increased Ki67 indices in rodent mammary models [41]. In contrast, RJ co-treatment reduced mammary Ki67 expression from severe to moderate, confirming earlier findings that RJ's antioxidant and anti-apoptotic actions in reducing proliferative signaling in chemically stressed mammary epithelium [7]. In skin, DMBA elevated Ki67 to moderate, matching observations that PAH initiation triggers keratinocyte hyperplasia [42]. Similar to mammary gland, RJ decreased skin Ki67 expression from moderate to mild reflecting its partial normalization of epidermal proliferation, which was in line with a study showing RJ attenuates wound-induced keratinocyte proliferation [43]. Notably, RJ's dampening of Ki67 was more pronounced in mammary tissue than in skin, suggesting tissue-specific sensitivity to RJ's modulatory effects. This difference may arise from distinct local microenvironments. Specifically, mammary epithelium under DMBA stress relies heavily on oxidative/apoptotic pathways, which RJ mitigates, whereas skin keratinocytes also engage wound-healing growth factors that RJ may partially sustain [44]. Collectively, these data confirm that RJ reduces DMBA-induced

hyperproliferation, with a stronger histoprotective outcome in mammary gland relative to skin.

Histologically, control and RJ groups displayed normal lobuloalveolar architecture in mammary tissue with no vacuolar changes, mitotic figures, necrosis, or corpora amylacea. DMBA caused vacuolar degeneration of epithelial cells, a substantial increase in mitotic figures, focal necrotic areas, and sporadic corpora amylacea within dilated ducts and lobules. Corpora amylacea are eosinophilic, laminated, glycoproteinaceous bodies typically associated with chronic stress or ductal obstruction in glandular tissue [35]. Their presence in DMBA-treated rats suggests sustained epithelial injury and lysosomal activity. RJ co-treatment ameliorated these changes, such as reducing vacuolar degeneration, mitotic figures, and necrotic foci. The reduction in corpora amylacea further indicates RJ's capacity to mitigate chronic cellular stress. These histological improvements reflected the combined antioxidant and anti-apoptotic actions of RJ by preventing ROS-mediated DNA damage and suppressing pro-apoptotic signaling, which confirmed RJ can maintain epithelial integrity and reduces necrosis. Moreover, RJ's estrogenic-like compounds may contribute to preserving ductal epithelial homeostasis under genotoxic stress [34, 35]. However, the incomplete restoration of normal histology suggests that RJ's protective mechanisms may not fully counteract DMBA's DNA-adduct formation and alkylation damage. Long-term studies would be required to assess whether histological normalization persists or if preneoplastic changes re-emerge after cessation of treatment. Regarding the skin tissue, the control and RJ groups exhibited normal epidermal thickness, intact dermal structure, and absence of mitotic figures, follicular hyperplasia, or necrosis. DMBA induced epidermal hyperplasia, elongation of rete ridges, mild desmoplasia, increased mitotic figures, hair follicle hyperplasia, and focal dermal necrosis. Epidermal hyperplasia reflects keratinocyte proliferation as an early preneoplastic event, responding to DNA damage and inflammatory signals [33, 38]. Hair

follicle hyperplasia is often observed in DMBA-initiated skin as follicular stem cells attempt repair but may also indicate dysregulated proliferation.

RJ co-treatment intensified skin proliferative changes, including reduction of mitotic figures, hair follicle hyperplasia, and necrosis. This observation may arise from RJ's pro-regenerative properties. It was reported that RJ accelerated epidermal regeneration and hair follicle proliferation in excisional wound models by increasing keratinocyte growth factor and vascular endothelial growth factor.

Conclusion

This study demonstrated that RJ exerts significant protective effects against DMBA-induced oxidative stress and apoptosis in rat mammary gland and skin. It restored antioxidant enzyme activity, rebalanced Bax/Bcl2/p53/Caspase-3 expression, and improved histological architecture. These findings highlight RJ's potential as an adjuvant antioxidant therapy, particularly for glandular tissues under chemical stress. Future studies should explore RJ's bioactive components, dose-response effects, and long-term safety in carcinogen-exposed tissues.

Limitations

Only one RJ concentration and DMBA dose were examined; dose–response studies are needed. We did not assess lesion progression to neoplasia. Extended follow-up with tumor incidence, latency, and malignancy grading is imperative. Due to the observed potential of RJ, it is suggested to conduct dose-response and long-term studies with more molecular pathway elucidation.

Declarations

Conflict of Interest

The authors declare that they have no financial, personal, or professional conflicts of interest that could influence the work presented in this document.

Data Availability

Data are available upon request from the corresponding author.

Ethics

All experiments were conducted following the International Council for Laboratory Animal Science guidelines. Additionally, the ethical approval for the study was granted by the Research Ethics Committees of Shiraz University of Medical Science with the approval ID IR.SUMS.REC.1404.402.

Consent to Participate declaration

Not applicable.

Funding

No funding source has impacted the objectivity or integrity of this work.

Authors' contributions

Alireza Salehi and Fatemeh Yaghoobi: Conceptualization, Methodology, Software, Writing original draft preparation, and investigation.. Seyed

Mohammad Hosseini: Data curation and Visualization. Seyedeh-Sara Hashemi: Supervision, Software, Validation.

Clinical trial number

Not applicable.

Consent to Publish declaration

Not applicable.

References

1. Hakkak, R. and S. Melnyk, *Soy protein diet changes metabolic profile in liver of 7, 12-dimethylbenz (α) anthracene (DMBA)-induced mammary tumors in obese zucker rats.* Cancer Research, 2024. **84**(6_Supplement): p. 759–759.
2. Lim, E.L. and J. DeGregori, *The Nature and Nurture of Carcinogenesis.* Cancer Discovery, 2025. **15**(6): p. 1090–1092.
3. Conney, A.H., *Induction of microsomal enzymes by foreign chemicals and carcinogenesis by polycyclic aromatic hydrocarbons: G. H. A. Clowes Memorial Lecture.* Cancer research, 1982. **42**(12): p. 4875–4917.
4. Kensler, T.W., et al., *Aflatoxin: a 50-year odyssey of mechanistic and translational toxicology.* Toxicological sciences, 2011. **120**(suppl_1): p. S28–S48.
5. Das, I. and T. Saha, *Effect of garlic on lipid peroxidation and antioxidation enzymes in DMBA-induced skin carcinoma.* Nutrition, 2009. **25**(4): p. 459–471.
6. Calaf, G.M., et al., *Protective role of curcumin in oxidative stress of breast cells.* Oncology reports, 2011. **26**(4): p. 1029–1035.
7. Mohamed, H.K., et al., *Anti-inflammatory, anti-apoptotic, and antioxidant roles of honey, royal jelly, and propolis in suppressing nephrotoxicity induced by doxorubicin in male albino rats.* Antioxidants, 2022. **11**(5): p. 1029.
8. Skrajnowska, D., et al., *Copper and resveratrol attenuates serum catalase, glutathione peroxidase, and element values in rats with DMBA-induced mammary carcinogenesis.* Biological trace element research, 2013. **156**: p. 271–278.
9. Elmore, S., *Apoptosis: a review of programmed cell death.* Toxicologic pathology, 2007. **35**(4): p. 495–516.
10. Chan, T.K., et al., *Polycyclic aromatic hydrocarbons regulate the pigmentation pathway and induce DNA damage responses in keratinocytes, a process driven by systemic immunity.* Journal of Dermatological Science, 2021. **104**(2): p. 83–94.
11. Ayala, A., M.F. Muñoz, and S. Argüelles, *Lipid peroxidation: production, metabolism, and signaling mechanisms of malondialdehyde and 4-hydroxy-2-nonenal.* Oxidative medicine and cellular longevity, 2014. **2014**(1): p. 360438.
12. Bergmann, A. and H. Steller, *Apoptosis, stem cells, and tissue regeneration.* Science signaling, 2010. **3**(145): p. re8–re8.
13. Pavel, C.I., et al., *Biological activities of royal jelly-review.* Scientific Papers Animal Science and Biotechnologies, 2011. **44**(2): p. 108–108.
14. Khazaei, M., A. Ansarian, and E. Ghanbari, *New findings on biological actions and clinical applications of royal jelly: a review.* Journal of dietary supplements, 2018. **15**(5): p. 757–775.
15. Vazhacharickal, P.J., *A review on health benefits and biological action of honey, propolis and royal jelly.* J. Med. Plants Stud, 2021. **9**(5): p. 1–13.
16. Aslan, A., et al., *Royal jelly arranges apoptotic and oxidative stress pathways and reduces damage to liver tissues of rats by down-regulation of Bcl-2, GSK3 and NF-κB and up-regulation of caspase and Nrf-2 protein signalling pathways.* Biomarkers, 2023. **28**(2): p. 217–226.

17. Karadeniz, A., et al., *Royal jelly modulates oxidative stress and apoptosis in liver and kidneys of rats treated with cisplatin.* Oxidative medicine and cellular longevity, 2011. **2011**(1): p. 981793.
18. Beigom Hejazian, L., S.M. Hosseini, and A. Salehi, *Neuroprotective Effects of Rosa damascena Extract against Aluminum Chloride-Induced Brain Damage in Rat Offspring.* Neurology Research International, 2023. **2023**(1): p. 5342849.
19. Shakib Khoob, M., S.M. Hosseini, and S. Kazemi, *In vitro and in vivo antioxidant and anticancer potentials of royal jelly for dimethylhydrazine-induced colorectal cancer in Wistar rats.* Oxidative Medicine and Cellular Longevity, 2022. **2022**(1): p. 9506026.
20. Wang, X., T. Yuwen, and T. Yanqin, *Mangiferin inhibits inflammation and cell proliferation, and activates proapoptotic events via NF-κB inhibition in DMBA-induced mammary carcinogenesis in rats.* Journal of Environmental Pathology, Toxicology and Oncology, 2021. **40**(2).
21. Wellington, D., I. Mikaelian, and L. Singer, *Comparison of ketamine–xylazine and ketamine–dexmedetomidine anesthesia and intraperitoneal tolerance in rats.* Journal of the American association for laboratory animal science, 2013. **52**(4): p. 481–487.
22. Percie du Sert, N., et al., *The ARRIVE guidelines 2.0: Updated guidelines for reporting animal research.* Journal of Cerebral Blood Flow & Metabolism, 2020. **40**(9): p. 1769–1777.
23. Valaei, A., et al., *Antioxidant and Anticancer Potentials of the Olive and Sesame Mixture against Dimethylhydrazine-Induced Colorectal Cancer in Wistar Rats.* BioMed Research International, 2022. **2022**(1): p. 5440773.
24. Weiss, S.L. and C.S. Deutschman, *Elevated malondialdehyde levels in sepsis-something to'stress' about?* Critical Care, 2014. **18**: p. 1–2.
25. Krishnamurthy, H.K., et al., *Oxidative stress: fundamentals and advances in quantification techniques.* Frontiers in Chemistry, 2024. **12**: p. 1470458.
26. Pei, J., et al., *Research progress of glutathione peroxidase family (GPX) in redoxidation.* Frontiers in pharmacology, 2023. **14**: p. 1147414.
27. Jafari, A., et al., *Effect of exercise training on Bcl-2 and bax gene expression in the rat heart.* Gene, Cell and Tissue, 2015. **2**(4).
28. Saaed, H.K., M.A. Mahmood, and N. Khoshnaw, *Quantitative real time PCR analysis of apoptotic gene expression in chronic lymphocytic leukemia patients and their relationships with chemosensitivity.* Applied Cancer Research, 2017. **37**: p. 1–7.
29. Salehi, A., S.M. Hosseini, and S. Kazemi, *Antioxidant and Anticarcinogenic Potentials of Propolis for Dimethylhydrazine-Induced Colorectal Cancer in Wistar Rats.* BioMed Research International, 2022. **2022**(1): p. 8497562.
30. Saxena, R. and A.J. Darnell, *Proliferation in the normal gastrointestinal tract: an immunohistochemical study with Ki-67.* Journal of Histotechnology, 2012. **35**(1): p. 22–26.
31. Salehi, A., S.M. Hosseini, and S. Kazemi, *Propolis ameliorates renal, liver, and pancreatic lesions in Wistar rats.* Biotechnology and Applied Biochemistry, 2024.
32. Rahimi, O., et al., *Hepatorenal protective effects of hydroalcoholic extract of Solidago canadensis L. against paracetamol-induced toxicity in mice.* Journal of Toxicology, 2022. **2022**(1): p. 9091605.

33. Beyaz, S., et al., *Fullerene C60 protects against 7, 12-dimethylbenz [a] anthracene (DMBA) induced-pancreatic damage via NF-κB and Nrf-2/HO-1 axis in rats.* Toxicology Research, 2023. **12**(5): p. 954–963.
34. Stevanović, J., et al., *Bee-inspired healing: apitherapy in veterinary medicine for maintenance and improvement animal health and well-being.* Pharmaceuticals, 2024. **17**(8): p. 1050.
35. Malkoç, M., et al., *The effects of royal jelly on the oxidant-antioxidant system in rats with N-methyl-N-nitrosourea-induced breast cancer.* Turkish Journal of Biochemistry, 2018. **43**(2): p. 176–183.
36. Baptista, B.G., et al., *Royal jelly: a predictive, preventive and personalised strategy for novel treatment options in non-communicable diseases.* EPMA Journal, 2023. **14**(3): p. 381–404.
37. Rizki, A.M.F., et al., *Effect of royal jelly to deal with stress oxidative in preconception women: A literature review.* Gaceta Sanitaria, 2021. **35**: p. S288–S290.
38. Sindi, A.A., *Thymoquinone decreases oxidative DNA damage (8-OHdG) in DMBA treated female Sprague Dawley rats.* 2013.
39. Yin, C., et al., *Bax suppresses tumorigenesis and stimulates apoptosis in vivo.* Nature, 1997. **385**(6617): p. 637–640.
40. Knudson, C.M., et al., *Bax accelerates tumorigenesis in p53-deficient mice.* Cancer research, 2001. **61**(2): p. 659–665.
41. Hamza, A.A., et al., *Salvadora persica attenuates DMBA-induced mammary cancer through downregulation oxidative stress, estrogen receptor expression and proliferation and augmenting apoptosis.* Biomedicine & Pharmacotherapy, 2022. **147**: p. 112666.
42. Lin, Y., et al., *The in vitro and in vivo wound-healing effects of royal jelly derived from Apis mellifera L. during blossom seasons of Castanea mollissima Bl. and Brassica napus L. in South China exhibited distinct patterns.* BMC Complementary Medicine and Therapies, 2020. **20**: p. 1–13.
43. Balmain, A. and S.H. Yuspa, *Milestones in skin carcinogenesis: the biology of multistage carcinogenesis.* J Invest Dermatol, 2014. **134**(e1): p. E2–7.
44. Yapar, K., et al., *Protective effect of royal jelly and green tea extracts effect against cisplatin-induced nephrotoxicity in mice: a comparative study.* Journal of Medicinal Food, 2009. **12**(5): p. 1136–1142.